Experiments with an Adaptable-Wall Wind Tunnel for Large Lift

Daniel C. L. Lee* and William R. Sears†
University of Arizona, Tucson, Arizona

Experiments have been carried out in a demonstration wind tunnel of the adaptable-wall type designed for the testing of high-lift configurations, such as powered-lift V/STOL aircraft. The simulated flight vector makes a large angle (30–40 deg) relative to the tunnel axis, so that the model's wake lies in a benign position. Simulation of flight at the desired speed and angle is accomplished by iteratively matching conditions at an interface within the tunnel to the calculated, updated outer flowfield. Measurements were made with a traversing laser-Doppler-anemometer system. The test model in these experiments was a V/STOL transport aircraft model with lower-surface blown wing flaps. Under test conditions, the powered wing-wake made a large angle with the flight direction, and wake positions were measured and are shown. Results show that the iterative procedure successfully reduced matching discrepancies at the interface. Typically, the best match was reached after about six or eight iterations, and this match represents precise simulation at the model to within 1% of stream speed.

Introduction

THE adaptable-wall wind-tunnel idea dates from the early 1970s.[1,2] It was an invention intended to solve a persistent problem of wind-tunnel testing, namely, boundary interference. The effects of boundaries can be corrected in many wind-tunnel tests at low or moderate speeds, but they cannot be corrected in nonlinear regimes, such as the transonic and the regime of very large lift.

In briefest outline, the adaptable-wall scheme consists of modifying the tunnel's geometry by an adjustment of the "wall controls," so as to produce the correct unconfined flow within the working section in the presence of the model. This is accomplished by measuring two independent flow-variable distributions at an interface that encloses the model, calculating the outer flowfield exterior to this interface (based on the measured values), and progressively reducing the matching-discrepancy at the interface by actuation of the wall controls.

It is clear that when the experimental (inner) and calculated (outer) fields are matched at the interface, the entire field is correct as the outer flow is always made to satisfy the far-field boundary conditions, namely, the freestream conditions, and the model enforces its own boundary conditions in the tunnel.

Thus, an adaptable-wall tunnel needs three special features: wall controls, instrumentation to measure the two distributions at the interface, and computer capability to calculate the outer flow for given boundary values at the interface. Several such tunnels, operating in the transonic regime, have been constructed in various countries. A progress report has been given in Ref. 3.

The adaptable-wall scheme also replaces the customary "calibration" of a wind tunnel; the determination of the stream vector (i.e., the negative of the flight-velocity vector) is made by choosing this vector in the outer-flow calculation and carrying out the elimination of the matching-discrepancy. This may be the most important feature of the adaptable-wall tunnel, since the traditional "calibration," which is carried out with an empty tunnel and then used for tests of models, is notoriously unreliable in both principle and practice.

As has already been mentioned, besides the transonic flight regime, another nonlinear regime in which difficulties in wind-tunnel testing are encountered is that of very large lift, as typified by the low-speed V/STOL regime and powered lift. Here it is principally the floor and ceiling of the working section that interfere with the highly deflected airstream and, especially, the powered, vortical wake. There is extensive literature concerning attempts to solve this problem. (See Ref. 4 and the papers cited therein.)

The program of research reported here was undertaken to see whether this persistent problem of the low-speed, high-lift regime could be solved by exploitation of the adaptable-wall strategy. Numerical simulations of wind-tunnel tests of high-lift configurations showed that the interface could be a five-sided box with open downstream end and with the vortical wake extending downstream through the open end. The sides of the interface were modeled as distributed-vortex panels, which have trailing vortices running back from their lateral edges, so that the interface is essentially semi-infinite in length. This made it unnecessary to try to locate the wake and to model it in the outer-flow calculation.

Next, it was ascertained that the freestream direction could be chosen to make a large angle, such as 40 deg, to the nominal "tunnel axis," and the scheme of iteration could successfully reduce the matching-discrepancy at the interface to negligible values. The results of these studies were published in Refs. 5 and 6, where a radically new type of wind tunnel, which seemed to offer a solution to the high-lift testing problem, was proposed. It would be an adaptable-wall tunnel in which the freestream vector would be sharply inclined with respect to the tunnel floor and controlled by the adaptable-wall principle. The test model would be mounted nose-down to give the desired angle of attack; consequently, the powered vortical wake would trail harmlessly downstream, essentially horizontally. The present program is an effort to demonstrate in a laboratory environment that the concept is sound.

The principle used in devising this tunnel, which divorces the flight direction from the architecture of the laboratory and the wind tunnel, would seem to have more applications than just the testing of high-lift aircraft configurations. It could also be applied to other cases where it may be more convenient to change angles of pitch and yaw by rotating the

Received Sept. 27, 1986; revision received Nov. 28, 1986.

*Research Assistant.
†Professor of Aerospace and Mechanical Engineering. Honorary Fellow AIAA.

freestream vector than by rotating the model. Nevertheless, the investigations reported here are confined to the testing at zero yaw of a typical high-lift airplane model with blown flaps.

Since the major goal of this research has been the proof of the concept, no effort was made to produce a facility suitable for routine testing. Neither the instrumentation nor the wall controls is "on-line." The working section is 20×20 in. in cross section. Tunnel speed can be about 70 knots (maximum), but its magnitude, within reason, is not considered to be important. Moreover, three important simplifications have been introduced, which have greatly reduced both the cost and complication of this project.

First, no balance system has been provided. This decision was based on the conviction that the basic principles of the adaptable-wall scheme have been verified in other embodiments (principally in the transonic regime). Thus, success in iterating to unconfined-flow conditions is measured by the matching-discrepancy distribution, rather than by any attempt to compare test results with results obtained with the same model in a very large tunnel or any other "exact" or "target" results. Clearly, it would be a major extension of this work to obtain such "target" results.

Next, since balance readings are not available, lift coefficients produced in these tests can only be estimated. Moreover, operating values of the overall "jet-flap coefficient" for the model are not precisely known. Instead of accurate values of these parameters, it is proposed that experimentally observed jet-wake geometries be understood to characterize the high-lift regime of the tests. Geometries were measured and are presented here. This characterization should be more significant to the reader in evaluating the success of the tunnel scheme than precise knowledge of lift and jet coefficients would be. The tunnel is intended to permit testing of large-deflection flows, especially those with powered wakes, rather than flows at any particular lift coefficient or jet-flap coefficient.

Finally, the working section was provided with only a relatively small number of wall controls. There were only 18 controls in all: 16 vaned panels, of which the vane angles can be varied between closed and full open, a variable-angle nozzle leading from the settling chamber to the working section, and a throttling device downstream of the working section, which controls the pressure differences across the top and bottom vaned panels. No controls were provided on the side walls. According to numerical simulations, this array of controls should be adequate to reduce the discrepancy function to satisfactorily small values.

Besides proof of concept, a major goal of this research is the demonstration of laser-Doppler anemometry as an instrumentation system for adaptable-wall wind tunnels in the fully three-dimensional application. Success in this demonstration confirms the positive results already achieved at the Ames Research Center[7]. Other goals have been the preliminary determination of the performance of wall-control panels consisting of adjustable vanes and the preliminary determination of the accuracy of attainment of unconfined flow and simulation of flows pertaining to selected freestream vectors in wind tunnels of this type.

Equipment

Wind Tunnel

The tunnel used in these investigations is shown in Fig. 1. It is an open-return tunnel, powered by a three-phase, induction motor, rated 25 hp at 1765 rpm, which drives a ventilating blower through a belt drive. The blower is rated at 18,200 ft^3/min at 1695 rpm. Nominal tunnel airspeed is controlled by adjustment of an inlet valve upstream of the blower. This motor/blower combination is observed to run accurately at constant speed (1640 blower rpm plus or minus 4) in all the experiments reported here, regardless of inlet-valve position, model configuration, or settings of the wall controls.

As seen in Fig. 1, the nozzle leading air from the settling chamber into the working section is adjustable in angle; this is one of the "wall-control" organs. Through an extension of the settling chamber, air is also admitted to the working section through control panels in its floor. There are eight panels in the floor and eight in the ceiling. These are rectangular panels made up of vanes of ⅝-in. chord. The vane angle of each panel is variable in angle from fully closed to about 75 deg open. At the downstream end of the working section (Fig. 1), there is an 18th control organ, namely, a valve made up of flat aluminum-alloy plates of 3-in. chord, which are turned in alternating directions so as to throttle the airflow. Each of the vaned panels as well as the downstream valve are controlled by a vernier dial/rotator that drives the vane angle through a worm drive. In these, the accuracy is controllable to approximately 1/10 deg.

Total-pressure measurements made in the empty working section, with controls set to produce 30- to 40-deg flow inclination, revealed that screens were required to equalize the total pressures of air coming through the nozzle and the floor panels. A combination of screens was found that minimized the total-pressure differences and also made the flow in the working section more steady. These screens were permanently installed. Total-head surveys carried out over a transverse plane just upstream of the test model, with model and controls set for a high-lift configuration, confirmed uniformity to within 1%.

Instrumentation

Instrumentation consists primarily of a laser-Doppler-anemometer system (LDA) based on a 2-W argon-ion laser, optical components and counter, and a traversing frame that moves the focusing lens and appropriate mirrors in three mutually perpendicular directions. It is a single-component

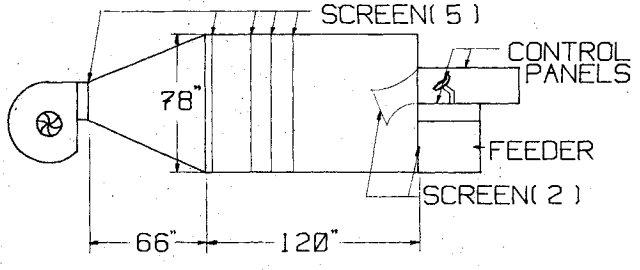

Fig. 1 Drawing of the wind tunnel. The working section (far right) is $20 \times 20 \times 57$ in.

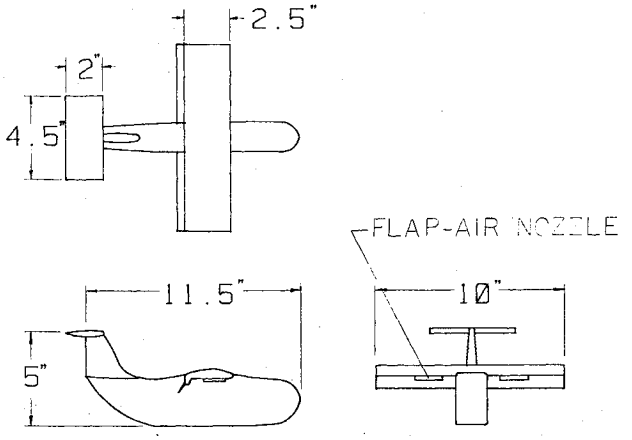

Fig. 2 The test model.

backscatter system. The laser is fixed in position, together with the collimator, polarization rotator, beam-steering module, beam splitter, signal receptor, and photomultiplier. The rest of the optical system, namely three mirrors and the focusing lens, is mounted on the traversing frame. Thus the measuring volume is translated in three mutually perpendicular directions, say x, y, and z. Measurement of two velocity components is accomplished by manually rotating the beam-splitter assembly.

A liquid seed consisting of 80% water and 20% glycerine, introduced into the flow at the blower intake, produced a satisfactory backscatter signal with indicated laser output of one watt. From the photomultiplier, the backscattered signal goes into a counter; thence, via an interface, into a microcomputer.

Test Model

All runs reported here were made with a "generic" STOL airplane model installed. This model (Fig. 2), represents a high-wing transport airplane with lower-surface-blown wing flaps. Its span is half of the tunnel width. Although its flaps are full span, they are blown by flat nozzles mounted on the wing lower surface, which directly affect only the inboard part of the wing. Flap blowing air is piped to the model from the laboratory's compressed-air system through the model-support strut. Pressure gages are installed in this air line to monitor both the supply pressure and the pressure drop across an orifice in the line. All experiments reported in this paper were made with flaps deflected to 60 deg and with a given, constant compressed-air pressure.

Tuft surveys showed clearly that, at high angles of attack, with flaps deflected to 60 deg, the wing is completely stalled, without flap air. When flap air is provided, the wing and flaps are unstalled inboard—at least 60% of the half-span—but still violently stalled outboard.

Procedures

Measurement of Velocity Components

The flow in the working section of this demonstration tunnel, with the model at the high-lift conditions described above, is grossly deflected and unsteady. This is characteristic of the high-lift, partially stalled regime, and, therefore, the measurement of time-averaged quantities is necessary to obtain meaningful data. Test procedures have been developed to measure mean values, averaged over a long enough time span to represent statistically steady values. Each reading reported here represents the average of at least 100 samples. (The word "sample" is used here to mean a signal accepted by the counter.) It required, typically, about 45 s to obtain such an average of 100 samples.

The Adaptable-Wall Algorithm

The logic of the adaptable-wall wind-tunnel scheme has been set forth in the Introduction. It has been converted into a detailed procedure and presented in several papers since it was first proposed in Refs. 1 and 2. (See Refs. 5 and 6.) The version used here follows Ref. 6.

Let f and g be two independent velocity-component distributions at the inner/outer flow interface, and let the subscript m denote measured values. Now let the notation $f[g]$ denote that a component distribution f, at the interface, is calculated for the outer field by using the component g, at the interface, as inner boundary data and satisfying the far-field boundary condition (uniform flow at a prescribed angle, in this case). For given f and g, the "mismatch" distribution at the interface is, say

$$f[g_m] - f_m = Df \tag{1}$$

The adaptable-wall strategy is to adjust the tunnel walls and tunnel speed, so as to add a fraction $k\ Df$ to the measured values f_m, where k is a "relaxation factor" less than 1, and to repeat the process iteratively until the mismatch is reduced to acceptable magnitude.

Introducing a superscript notation, namely letting superscript (p) denote values measured in the pth iteration $(p=1,2,\ldots)$, yields

$$D^{(p)}f = f[g_m^{(p)}] - f_m^{(p)} \tag{2}$$

and $f_m^{(p+1)}$ is adjusted, as closely as possible, to

$$f_m^{(p+1)}m = f_m^{(p)} + kD^{(p)}f \tag{3}$$

The procedure used to set the wall controls as required by Eq. (3) will be explained later.

The "Figure of Merit": RMS

In actual experiments it will always be impossible to drive the matching discrepancies, or mismatch values, at the interface to zero, because the number of control organs is finite, the modeling of the outer flow is approximate, and there are other sources of experimental error. The operator of an adaptable wind tunnel must therefore decide upon a "figure of merit" that is a measure of how good a match has been achieved, overall, at the surface, and must undertake to reduce the figure of merit to a minimum. In this investigation the root-mean-square matching error is used; namely, in the notation used above,

$$\text{rms} = \text{root-mean-square value of } Df$$

$$= \text{SQR}\left\{(1/N)\sum_{i=1}^{N}(Df_i)^2\right\} \tag{4}$$

where N is the number of field points.

The relationship between this figure of merit and the accuracy of simulation is discussed later in this paper.

Interface and Calculation of Outer Flow

The interface is the same as defined in Ref. 6, namely a rectangular box, semi-infinite in length (Fig. 3). (The coordinate system, x,y,z, is also shown.)

To calculate the outer flowfield, singularity panels are arrayed on the interface. These are distributed-vortex panels on the top, bottom, and sides of the interface and source panels on the front. The use of singularity panels requires that the velocity components f and g be redefined as *perturbations* measured from the far-field values of the appropriate velocity components. This does not involve any changes in Eqs. (1-4); it means that the far-field boundary values of f and g are zeros.

These perturbation velocity components, for the experiments reported here, have been defined as follows:

In all cases, g is the tangential perturbation at the center of the respective panel; thus, at the four front panels, g is the vertical (z) component, and at all other panels it is the x component. This component is usually referred to as "V_t."

In all cases, f is a combination of normal and tangential perturbations. At the four front panels it is the normal (x) component at panel center; at the 16 top and bottom panels, it is the normal (z) component at panel center; at the 12 side panels, it is the x component at a point 1 in. outboard of the panel center. This component is referred to as "V_e."

For the outer flowfield defined by these singularity panels, the calculation designated by $f[g]$, above, consists merely of a matrix multiplication; namely,

$$V_e[V_t] = EB^{-1}\ V_t \tag{5}$$

where E and B are the 32×32 matrices described above, relating V_e and V_t to the panel strengths, and B^{-1} is the in-

verse of B. The procedure, of course, has been to construct the square matrix EB^{-1} and provide it on working disks; it is a function of interface geometry only.

Control Matrix and Calculation of Control Settings

A crucial step in the adaptable-wall algorithm is the one represented by Eq. (3), namely, the process of altering the measured velocity components, by adjustment of the wall controls, so as to reduce the matching discrepancy at the interface. The procedure for this step is to measure the matrix of control effects and undertake to calculate the array of control increments required to satisfy Eq. (3). Specifically, since $D^{(p)}f$ in Eq. (2) represents $D^{(p)}V_e$, the matrix that relates increments of V_e to increments of control settings is measured.

In general, one must expect that control effects are dependent upon the existing flow in the working section and, therefore, upon both the model configuration and the existing control settings. To employ a control-effect matrix (or, presumably, any other computational procedure) at this point must imply that the increments involved will be small enough to permit local linearization of the process.

Under the assumption that this local linearization is possible, an experiment is carried out in which each control organ, in turn, is given a small increment and the resulting increments of V_e at all the field points of the interface are measured. The result is an $N\times M$ matrix, where N is the number of field points and M the number of controls; its members are the increments of V_e resulting from unit, positive increments of control settings. For the vaned-panel controls, unit deflection is about one-tenth the available vane angle, or about 7.5 deg. The difference from which the matrix member is computed is centered on the nominal control setting. Strictly, each control matrix measured in these experiments pertains to a given model configuration, including angle, and a given array of control settings, but it is expected that such a matrix has validity over a reasonable range of control settings, as mentioned above.

For the full tunnel, N is 32 and M is 18, as has already been pointed out; however, most of the experiments were made with laterally symmetrical model configurations and under the assumption of laterally symmetrical flow, as will be explained below, so that N and M were 16 and 10, respectively. In either case, N is greater than M; hence M control settings are overdetermined by N values of kDV_e. The control settings are then calculated to give the best fit—i.e., the least mean-square error—to the desired values. If the result of this "inversion," an $M\times N$ matrix, is called Y, the formula for the array of control increments required by Eq. (3) becomes

$$\text{Control Increment} = YkDV_e \tag{6}$$

For practical reasons, all of the computations and manipulations described in this report are carried out in terms of V_e and V_t, *perturbations* of the far-field values of the respective velocity components, as has already been pointed out, whereas the components measured by the LDA are actual total velocity components. The values of the unperturbed (stream) velocity components U and W into the computer at the beginning of each run. When both components were recorded at the last field point, the program proceeded to calculate the outer perturbation flow and to evaluate and print out the distribution DV_e and rms. Then, unless interrupted, it used the inverted control matrix called Y, above, and then calculated and printed the control increments and resulting control settings for a next iteration.

Clearly, any set of measured data (velocity components) can be interpreted as perturbations from any chosen stream components. In other words, a search can be carried out, varying the two parameters U and W, and a smallest rms found, for any given set of data (any given run). This search consists simply of adding constant increments to V_t and V_e and recalculating DV_e and rms. For most runs, such searches were carried out, and in some cases small changes of U and W were introduced. This minor modification of the adaptable-wall procedure was often found to accelerate convergence.

The Assumption of Lateral Symmetry

When the wind tunnel and the model configuration are both laterally symmetrical, the resulting flow should exhibit the same symmetry, in which case measurements should only have to be made in one-half of the tunnel and the wall controls operated in pairs. This situation would afford considerable simplification of the experimental procedures and the processing of data. For example, control-effect matrices would become 16×10 instead of 32×18, with resulting great reduction of time required to measure them.

Most of the experiments reported here were carried out in that mode: The test volume was the east, say, half of the tunnel (where the stream direction is north); the measurements and calculations were directed toward control of the flow in that test volume; the west half of the tunnel possessed the same control and model configurations, but no data were taken to validate the accuracy of the simulation in the west half. It is believed, and verified experimentally, that the same techniques that succeed in the half-tunnel also succeed in the full 32×18 embodiment.

For the tests made in the full-tunnel, 32×18 mode, the term "asymmetric mode" is used, although the model configuration was always nominally symmetrical.

Wake Surveys

The procedure for "wake surveys" consisted simply of using a square-ended total-head tube to locate, approximately,

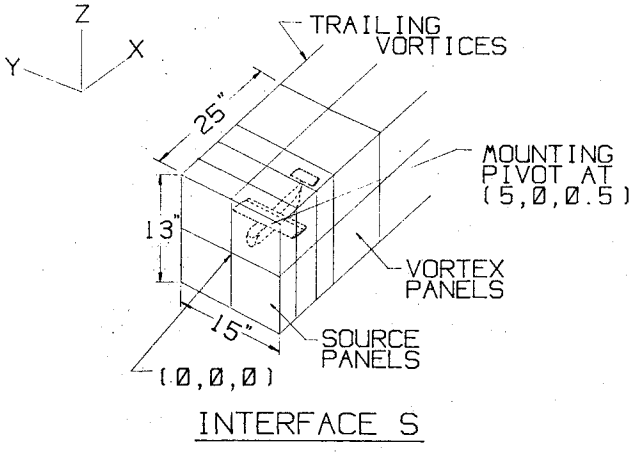

Fig. 3 Diagram showing interface, singularity panels, and coordinate system.

Table 1 Results of iterations[a]

Model angle, deg	Angle of attack, deg	Freestream Speed, m/s	Freestream Inclination, deg	Best rms, percentage of speed
−11	21	5.7	31.7	4.0
−18	21	7.2	39.1	3.6
−13	20	7.4	33.4	4.6*
−13	22	7.1	35.2	2.7
−19	21	2.6	39.6	4.0

[a]This experiment was carried out in the asymmetric mode. The other results listed were obtained in the symmetric mode.

the locus of maximum total head in a vertical plane 6.25 in. from the wall of the working section. It was easy to identify the maximum at locations back to about 11 in. behind the wing trailing edge; the jet wake was more diffuse farther aft. The LDA and its traverse system were used to locate the nose of the total-head tube.

Presentation of Results

Essentially four different kinds of experiments were carried out in the course of these investigations: measurement of control matrices, iterations toward desired flow conditions, runs at constant control settings and varying angle of attack, and wake surveys.

Control Matrices

There does not seem to be any useful and practical way to present the results of the matrix measurements in this paper. In Ref. 8, which is a more complete report on this research, bar graphs are presented that show all the matrix members for four symmetrical cases and one asymmetrical case. From those presentations, the following general conclusions are deduced:

The array of adjustable vane panels generally meets the requirements of controlling the flow at the interface; namely, all field points are affected by at least one control and no two controls affect all field points in a proportional way.

The matrices are not very sensitive to changes in test conditions such as angle of attack and undisturbed-stream inclination.

One of the control devices, namely, the adjustable-angle nozzle (see Fig. 1) is relatively ineffective.

Iterations

Detailed data from five series of iterations, representative of the results of this program, are presented in Ref. 8. Here, in Table 1, only the final results of five typical iterations are presented. In each case the iterations were begun with controls set arbitrarily, and the "best rms" values tabulated were arrived at after six to eight iterations, using a relaxation factor k of 0.15, after which further iterations failed to reduce rms.

Runs at Constant Control Settings, Varying Angle of Attack

These runs were made to explore the effect on rms of changing model angle without changing control settings. An important simplification of the test procedure would result if it were possible to iterate to a best setting at one angle of attack and then run through a range of angles without reoptimizing the control settings. Two series of such runs are summarized in Table 2.

These results suggest that the above-mentioned simplification may be acceptable. In both series of runs in Table 2 the control settings were optimized for the largest angle of attack.

Wake Geometries

In Fig. 4 are plotted the positions of the jet wake as measured in two experiments, i.e., the loci of maximum total pressure in the vertical plane 6.25 in. from the wall of the working section. Figure 4a, which shows the loci for both east and west sides, pertains to stream speed, flow inclination, angle of attack, and flap pressure typical of most of the experiments, as can be verified by reference to Table 1, above. Thus the wake geometry shown is typical. The energized wake leaves the trailing edge at an angle of about 60 deg to the freestream direction and would lie undesirably close to the floor in a conventional tunnel.

Figure 4b refers to an experiment, mentioned earlier, which is atypical in that the flap-blowing coefficient was increased by reducing stream speed (see Table 1). In this case

Table 2 Results of runs at constant control settings and varying angle of attack

Model angle, deg	Angle of attack, deg	Freestream Speed, m/s	Freestream Inclination, deg	Best rms, percentage of speed
−26	6	5.5	32.0	3.0
−21	11	5.5	32.0	3.7
−16	16	5.5	32.0	3.4
−11	21	5.5	32.0	3.8
−31	4	7.7	35.1	5.0
−25	10	7.7	35.4	5.0
−19	16	7.6	35.5	4.1
−13	23	7.4	36.4	3.6

Table 3 Mean absolute extraneous velocity component at model position (% of stream speed)

rms, %	V_x	V_z
4.0	0.9	1.2
3.6	1.5	0.6
4.6	0.9	0.4
2.7	1.0	0.5
4.0	0.1	0.4

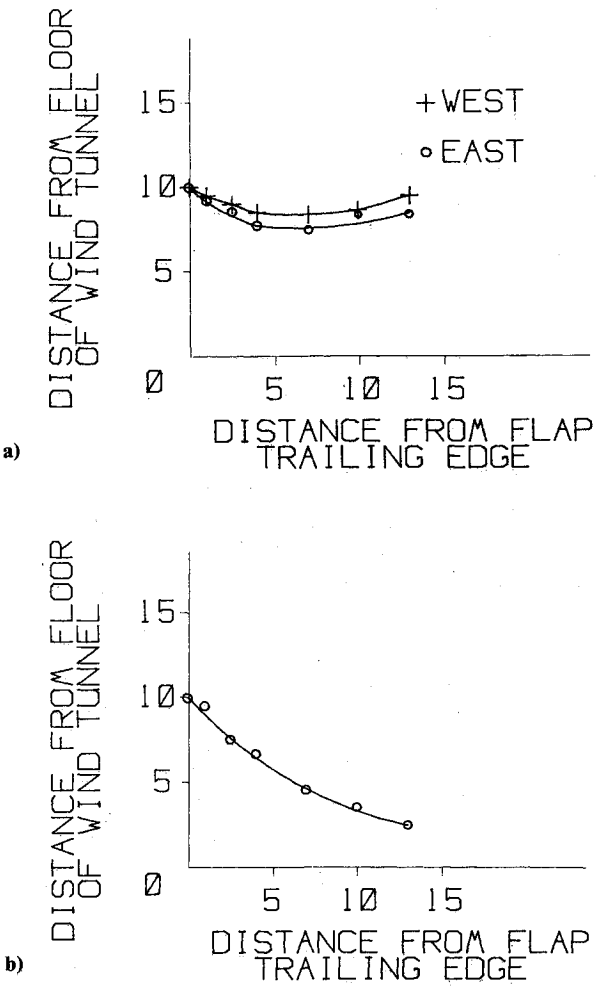

Fig. 4 Wake geometries: loci of maximum total pressure. a) Asymmetrical mode. Model angle = −13 deg, stream angle = 33.5 deg, nominal angle of attack = 20.5 deg. b) Symmetrical mode. Model angle = −19 deg, stream angle = 41 deg, nominal angle of attack = 22 deg.

the wake leaves the trailing edge at an angle greater than 80 deg. It seems that this experiment would be difficult or impossible to carry out in conventional tunnels.

Discussion

Up to this point, the success of the tunnel has been measured in terms of a rather arbitrary figure of merit, the rms matching discrepancy at the interface. It is interesting to explore the relationship between this figure of merit and the accuracy of simulation at the model.

Some data on this relationship can be obtained by a simple numerical calculation for representative cases. When a distribution of matching-error is present at the interface, the correct boundary conditions are satisfied, both in the far field and at the model, but there is a discontinuity at the interface. If an equal-but-opposite discontinuity is introduced at the interface, the flowfield will be continuous and will satisfy the far-field conditions, but conditions at the model will be disturbed by a field of extraneous velocities equivalent to changes of the model's geometry and/or angle of attack. Thus, an evaluation of the tunnel's accuracy can be obtained by introducing these discontinuities at the interface and calculating their field of velocities at the model position.

In the present case, when DV_e is known at the field points, the compensating discontinuity distribution consists of source-sink panels of strength $-DV_e$ at the top, bottom, and front field points, and distributed-vortex panels of strength $-DV_e$ at points 1 in. outboard of the side panels. Computer programs have been constructed to calculate the velocity field of this array of singularity panels, and these have been used to calculate the vertical and horizontal extraneous velocity components at points at the test model's position; namely, for symmetric cases, seven points, three along the wing quarter-chord line and one each at fuselage bow and stern, empennage, and in the near wake behind and below the wing trailing edge; for asymmetric cases, nine points, same, but with two more points on the quarter-chord line.

The results of the calculation are summarized in Table 3 for the five experiments reported in Table 1. The values shown, V_x and V_z are the absolute extraneous horizontal and vertical velocity components averaged over the seven (nine) points defined above. These results suggest that the accuracy of simulation achieved in the tunnel in these experiments was, typically, about 1% of stream speed.

This kind of accuracy in simulation is adequate for many wind-tunnel tests, especially in the high-lift regime. It may, in fact, be substantially better than is available in many tunnels. Nevertheless, better matching at the interface would surely improve the accuracy of simulation at the model; hence considerable time and effort have been devoted to studying the iteration process and the sources of the apparent limitation of matching accuracy. Such sources include inaccuracy of measurement of velocity components, limited number of controls, inaccuracies in the determination of control settings to achieve desired V_e introduced by the approximation of local linearity or by the inaccuracy of "best-mean-square inversion" of the control matrix.

Some information about the accuracy of measurement was obtained by carrying out repeated runs, the results of which should be identical. These data actually show that the inaccuracy is about 1% of stream speed. Thus, inaccuracies in the measurement of time-averaged velocity components were probably large enough to account for an important part of the observed "residual" rms.

It is certainly true that the availability of only 18 controls in an asymmetric case, or 10 in a symmetric case, limits the minimum rms. The decision to use such a modest number of controls—as well as the decision to forego side-wall control elements—was based upon the results of the computer simulations that preceded this experimental investigation (Refs. 5 and 6).

Evidence of linearity or nonlinearity of control effects was available during each matrix measurement; namely, it could be observed whether the increments of velocity due to positive and negative control increments were of nearly the same magnitude. This criterion was well satisfied, within the limits of accuracy discussed above, for most field points. It is believed that departure from local linear behavior was not a serious problem in this research.

The errors due to best-mean-square fitting in calculating control deflections were evaluated in several typical cases; the measured control matrix was used to calculate the expected V_e increments that should result from the calculated (approximate) control settings, and these were compared with the values desired. In every case the differences were very small—well within the experimental error. In other words, a best-mean-square fit to 32 points by 18 controls (or to 16 points by 10 controls) is a good approximation. This detail of the procedure is not one of the serious limitations.

Acknowledgment

This research was carried out under sponsorship of the U.S. Air Force Office of Scientific Research under Grant AFOSR-82-0185.

References

[1]Ferri, A. and Baronti, P., "A Method for Transonic Wind Tunnel Corrections," *AIAA Journal,* Vol. 11, Jan. 1973, pp. 63-66.

[2]Sears, W. R., "Self-Correcting Wind Tunnels," *Aeronautical Journal,* Vol. 78, Feb.-March 1974, pp. 80-89.

[3]Ganzer, U., "A Review of Adaptive Wall Wind Tunnels," *Progress in Aerospace Sciences,* Vol. 22, 1985, pp. 81-111.

[4]Parikh, P. C. and Joppa, R. G., "Numerical Simulation of a Controlled-Flow Tunnel for V/STOL Testing," *Journal of Aircraft,* Vol. 23, March 1986, pp. 186-191.

[5]Sears, W. R., "Wind-Tunnel Testing of V/STOL Configurations at High Lift," Proc. 13th Congress of ICAS, Seattle, Wash., Aug. 1982, pp. 720-730.

[6]Sears, W. R., "Adaptable Wind Tunnel For Testing V/STOL Configurations at High Lift," *Journal of Aircraft,* Vol. 20, Nov. 1983, pp. 968-974.

[7]Satyanarayana, B., Schairer, E., and Davis, S., "Adaptive Wall Wind Tunnel Development for Transonic Testing," *Journal of Aircraft,* Vol. 18, April 1981, pp. 273-279.

[8]Sears, W. R. and Lee, D. C. L., "Experiments in an Adaptable-Wall Wind-Tunnel for V/STOL Testing," Final Report submitted to U.S. Air Force Office of Scientific Research under Grant AFOSR-82-0185, University of Arizona, Tucson, AZ, Sept. 1986.